Northrop F-5A Aircraft Transonic Buffet Pressure Data Acquisition and Response Analysis

Chintsun Hwang* and W. S. Pi†
Northrop Corporation, Hawthorne, Calif.

Flight tests were performed on an extensively instrumented F-5A aircraft to investigate the dynamic buffet pressure distribution on the wing surfaces and the responses during a series of transonic maneuvers called the windup turns. The maneuvers were performed at three Mach number-altitude combinations with a constant q of approximately 14,360 N/m^2 (300 psf). The fluctuating buffet pressure data at 24 stations on the right wing of the F-5A were acquired by miniaturized semiconductor type pressure transducers mounted on the wing. A new transducer mounting and wiring technique was applied where the interference with the natural flow condition was minimized. The data acquired in this manner were found adequate to trace the shock origin, the movement of the shock front and the development of the separated flow (shock-induced or leading-edge induced) on the wing surface. An analytical procedure, called a "segmentwise stationary procedure," was introduced to compute the aircraft response spectra based on the measured buffet pressures. The analytical response data computed in this manner are correlated with the test response data obtained in the same flights.

Nomenclature

$A_{(\ )}$ = Fourier transform of the deterministic shaping function for various time segment
$b_r = \frac{1}{2}c$ = reference semichord
B_e = equivalent resolution bandwidth
c = geometric chord
$f = \omega/2\pi$ = frequency
$F_{(\ )}$ = Fourier transform of a function, $F_x(\omega) = 1/T \int_0^T x(t)e^{-i\omega t}dt$
G = gravitational acceleration
h = flight altitude
$I_{(\ )}$ = modal influence function for various time segment(s)
$k_r = \omega b_r / V$ = reduced frequency
M_0 = Mach number
n = total number of time segments
Q = time segment modal forces
t, τ = time
T = time span
V = flight velocity
w = structural deflection at a specific location
α = angle of attack
δ_n, δ_f = leading and trailing edge flap angles
ϵ = normalized standard error
ω = circular frequency
$\phi(\ )$ = one-sided spectral density function
i, j = location indices in Eq. (3); i, j also serve as modal indices of $H(\omega_j)$ and $I_r(t,\omega)$ in Eq. (7).
$(\ )^*$ = complex conjugate of a function

Matrix Conventions

$[\ ]$ = square or rectangular matrix
$\{\ \}$ = column matrix
$\lceil\ \rfloor$ = diagonal matrix
$\lfloor\ \rfloor$ = row matrix
$[\ ]^T$ = transposed matrix

Matrices

$\lceil A \rfloor$ = wing subarea matrix associated with pressure transducers
$\{f_{(\ )}\}$ = Fourier transforms of modal force matrix
$[H]$ = modal transfer function matrix
$[I_{(\ )}]$ = modal deflection influence function matrix
$\{P_{(\ )}\}$ = measured pressure matrix
$[S_{(\ )}]$ = two-sided spectral density matrix
$[X]$ = modal shape matrix corresponding to pressure transducer locations
$\lfloor Y \rfloor$ = modal shape matrix corresponding to locations where deformation and/or acceleration are computed
$\{\alpha_{(\ )}\}$ = Fourier transform of modal amplitudes

Received April 26, 1974; revision received January 24, 1975. The work described in this paper was carried out under contract NAS2-6475 sponsored by NASA Ames Research Center. The authors wish to acknowledge the enthusiastic support and constructive comments made by C. Coe and D. Buell of NASA/Ames throughout the program. The authors also acknowledge the excellent technical support rendered by Northrop Flight Testing Department under the capable direction of H. Pink.

*Manager, Structural Dynamics and Aeroelasticity Research, Structural Research and Technology Department, Aircraft Division.

†Engineering Specialist, Structures Research and Technology Department, Aircraft Division.

Introduction

BUFFET is a dynamic behavior of aircraft flying at a high angle of attack. It occurs in the transonic region where the aircraft has substantial forward speed, and the angle of attack becomes large because of certain maneuvers initiated by the pilot. The initial phase of buffet is called buffet onset when noticeable vibrations or oscillations are observed. When the angle of attack is further increased, the aircraft responds to the accumulated effects of the dynamic buffet pressures with large amplitude rigid body oscillations which are usually coupled with structural vibrations. This latter phenomenon of sustained, large-amplitude aircraft oscillation is called wing rock.

The work described in this paper deals with the flight test and data evaluations of the Northrop F-5A aircraft in transonic maneuver. A unique feature of the test program involves the extensive dynamic pressure instrumentation using miniaturized simiconductor-type transducers and a new installation technique. Both fluctuating buffet pressures and significant aircraft response data were recorded and spectral analyses were performed. Specifically, the data acquired in a small time segment of the maneuver were assumed to be stationary so that auto- and cross-power spectra could be generated. The display of a set of power spectra generated for various time segments of the maneuver yielded results that illustrated the various phases of the buffet phenomenon.

To complement the flight test results, work was carried out to correlate the response data using the measured buffet

Buffet Flight Test of F-5A

The F-5A used in the buffet test was a single-seat fighter capable of carrying stores at wing fuselage pylon stations. The buffet test was conducted with two wingtip stores; otherwise the wing was clean. A three-view drawing of the F-5A is shown in Fig. 1. The essential data of the wing are given in Table 1. In the buffet flight tests, both Pulse Code Modulation (PCM) and FM recording systems were used to record the flight condition, the dynamic pressures and selected response data.

To monitor the dynamic pressures, 24 miniaturized differential pressure transducers were installed on the right wing of the test aircraft. To minimize the interference to natural flow conditions, the transducers were mounted on the right wing surfaces flush with a 0.1016 cm (0.040 in) plexiglass jacket assembled in strips and bonded to the wing surfaces. The transducer locations and the areas covered by the Plexiglass are shown in Fig. 2 where the boundaries of the Plexiglass jacket are identified by heavy solid lines. Along the edges of the Plexiglass jacket, a 15:1 taper was cut to blend the jacket to the wing surface. Internally, the reference pressure tubings from all transducers were plumbed into a common manifold chamber inside the fuselage. All tubings and transducer wire harnesses were routed under the plexiglass jacket.

The basic maneuver used in the test program was the wind-up turn at constant Mach number. Specifically, wind-up maneuvers from level flight to maximum lift (in each run) were performed using 3 Mach number/altitude conditions; (0.75/7,772 m), (0.85/9,449 m) and (0.925/10,668 m). Various combinations of leading edge and trailing edge flap settings (retracted or extended) were maintained during the test maneuvers. Data were recorded from 1-G level flight through recovery from the maneuver.

Presentation of Real Time Data

The transonic maneuver was executed by a combined turn and roll motion at maximum thrust. The aircraft was allowed to lose altitude so that the Mach number was maintained. In a typical wind-up turn at the test altitude range, 7772-10,668 m (25,500-35,000 ft), the lost altitude was in the range of 152-305 m (500-1000 ft). During this time, the angle of attack was increased to a maximum value. As the angle of attack increased, the buffet onset was first encountered, detectable by instrumentation (e.g., accelerometer under the pilot seat) or by pilot perception. As the angle of attack reached its maximum, sustained structural vibration of the aircraft took place. The vibration was accompanied by severe rigid body oscillations such as the yaw and roll motions. The sustained rigid body oscillation is called wing rock. To terminate the maneuver, the pilot pushed the stick forward and returned the aircraft to a level position.

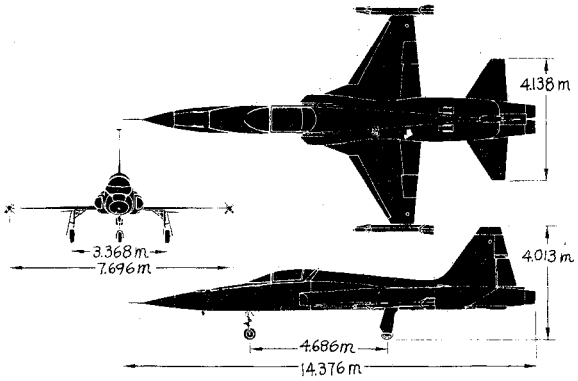

Fig. 1 Basic dimensions of F-5A.

Table 1 F-5A aircraft wing data

Airfoil section	NACA 65A004.8 (Modified)
Area (reference)	15.79 m^2 (170.00 ft^2)
Span (clean tips)	7.696 m (25.25 ft)
Aspect ratio	3.75
Taper ratio	0.20
Sweepback (25% chord)	24°
Mean aerodynamic chord	2.356 m (7.73 ft)
Dihedral angle	0
Incidence angle	0

Typical pressure data acquired in the tests are shown in Fig. 3 for pressure transducers 1-3 identified in Fig. 2. On top of Fig. 3, was noted the time counts, in seconds, as well as the instantaneous angle of attack data. Referring to the figure, as the angle of attack was increased, the first major noticeable pressure oscillation appeared at $t=073.0$ at Station 2. The pattern indicated oscillation of the shock front as a result of downstream separation during the maneuver. Downstream separation can be seen in the pressure fluctuation of Station 3. This can be defined as the buffet onset point. As the angle of attack was further increased (to approximately 6.2° at $t=0$ 76.0), the separation boundary (as defined by the shock front oscillation) moved to Station 1. It is worthy of noting that the pressure traces showed distinctly varied characteristics corresponding to local unseparated and separated flow conditions.

Based on real-time pressure data such as shown in Fig. 3, the flow separation boundaries on the upper wing surface may be traced. Figure 4 illustrated schematically the variation of the separation boundary with time. Referring to the figure, at $M=0.75$, the separated flow was leading edge induced. The separation boundaries seemed to follow a chordwise direction with some influence possibly due to the fuselage vortex front. For higher Mach numbers, especially at $M=0.925$, the separated flow was shock-induced. In the early stage of the maneuver, the separated flow boundary in the outer semispan area seemed to move from a certain chordwise position toward the leading edge. As the angle of attack was further increased, the separated flow region expanded toward the fuselage and eventually covered almost the complete upper wing surface.

Spectral and Statistical Processings

The transonic maneuver of an aircraft is transient in nature. The power spectra of the flight test data is computed based on the assumption that the dynamic data within a limited time segment is random and almost stationary. On the other hand, the normalized standard error ϵ of a spectral function is determined by

$$\epsilon = (B_e T)^{-1/2} \tag{1}$$

where B_e is the effective resolution frequency and T is the time span. Thus, the requirements of stationarity, a high degree of frequency resolution, and a minimum normalized standard error pose conflicting conditions on the processed data. It is then important to weigh these factors and to determine the most appropriate time span, sampling rate, and the resolution frequency(s) for spectral processing. In the subject program, a study was made by varying the processing parameters to ensure that the normalized standard error of the spectral data was within a reasonable range. Readers interested in this subject are referred to Ref. 18 where some numerical examples were presented.

The pressure data were processed and converted into power spectra for a wind up-turn at $M_0=0.75$ and $h=7{,}772$ m (Run 7, Flight No. 825). Figure 5 shows the pressure power spectra obtained at the top surface of Wing Station 128.31, 90% semispan and 90% chord position (Pressure Station 4, Fig. 2) for a separated flow condition. The power spectrum in the frequency range above 100 Hz seems to follow the -5/3 slope indicated by the inserted broken line. It is worthy of noting that the -5/3 slope is predicted by the theory of universal equilibrium in homogeneous turbulent flow.[16] The time span

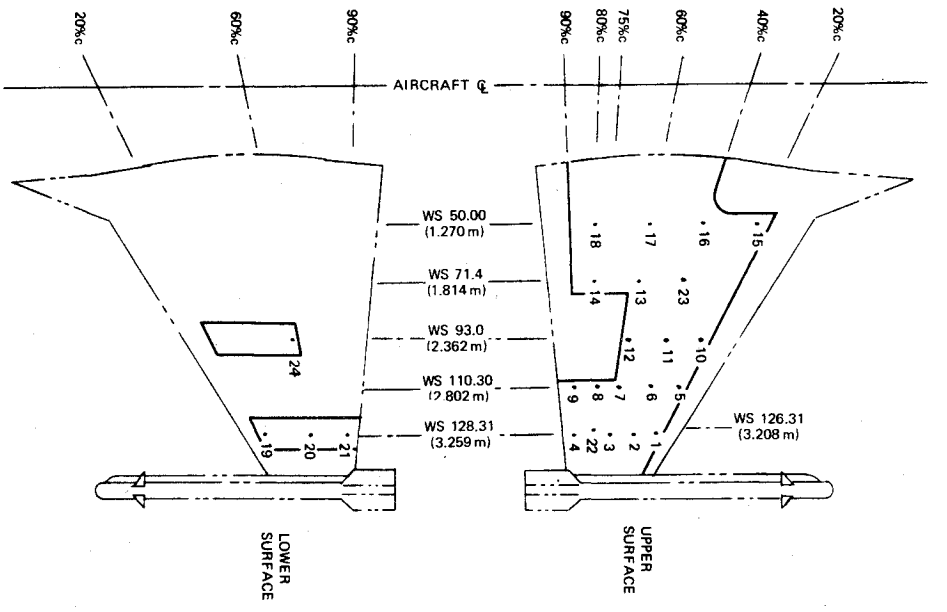

Fig. 2 Dynamic pressure transducer locations and the areas covered by the Plexiglass jacket on F-5A right wing.

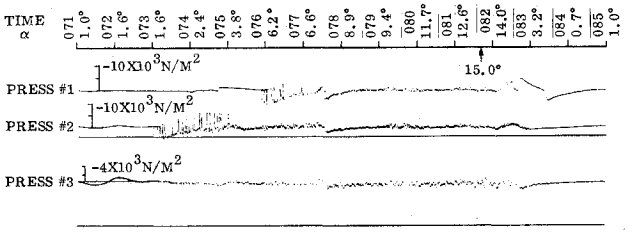

Fig. 3 Oscillagraphs of pressure station 1, 2, 3, recorded in run 2, flight 871. $M_0 = 0.925$, $h = 10{,}668$ m, $\delta_n = 4°$, $\delta_f = 12°$.

pressures. A nonstationary analysis procedure was used which predicted with a fair degree of success the time-varying aircraft responses at selected locations.

during which the spectral data of Fig. 5 were acquired was $t = 363.4 - 364.22$. During this time, the flow on the complete upper wing surface became separated. A typical power spectrum plot for an inboard pressure station located on the trailing edge flap, Pressure Station 18, Fig. 2, acquired at the same time interval is shown in Fig. 6. (All PSD plots in this paper are one-sided PSD's, even though two-sided PSD's are used in some later formulations.)

For data acquired in Run 5, Flight 825, ($M_0 = 0.925$, $h = 10{,}668$ m, $\delta_n/\delta_f = 0°/0°$), five time segments were chosen for spectral processing. Each time segment represented 1.025 sec. Roughly, the five time segments may be classified as in Table 2 (also see Fig. 4c).

The five PSD plots for each function corresponding to the time segments A-E are presented in a single figure. For Pressure Station 1, the PSD's are shown in Fig. 7. Referring to the figure, at time segment A, the flow at Station 1 was unseparated, the PSD level was at its minimum. In time segment B, the shock appeared and passed through the local station. The PSD showed drastic increase and reached its peak values of the complete maneuver. The PSD level subsided gradually in time segments C and D when the shock boundary moved inboard and the separated flow region expanded on the wing surface. The relatively high PSD level in time segment E was contributed to the high turbulence during wing rock and the turbulence caused by the transient recovery maneuver. For the same flight, the PSD's for the c.g. normal acceleration are given in Fig. 8. The corresponding right-hand aileron hinge moment PSD's are given in Fig. 9.

Aircraft Response Analysis

In order to improve the analytical correlation of aircraft response results, the major portion of a transonic maneuver is divided into a number of segments. In each segment, the buffet pressure data are assumed to be stationary. The aircraft is then subjected to the consecutive application of the buffet loads and the cumulative dynamic effects are reflected in the time varying PSD of response. The approach was applied to the set of flight test data in Table 3. Some of the real-time data of this run were given in Fig. 3. Altogether, dynamic pressure data covering the time span 073.00-082.10 sec are used. The data are divided into 4 equal time segments. The computation is carried out using the rigid body plunging mode and the first three symmetrical flexible modes. The pitch mode is not included because of lack of tail surface dynamic loads data.

The segmentwise stationary analysis starts with the PSD matrix of the modal forces f_r, f_s where r, s are time segment indices and f_r, f_s are column matrices themselves.

$$[S_{f_r f_s}(\omega)] = [X]^T \lceil A \rfloor [S_{p_r p_s}(\omega)] \lceil A \rfloor [X] \tag{2}$$

Table 2 Time segment definition of a transonic maneuver

Designation	Starting time	Initial	Description
A	334.0	2.2°	Initiated wind-up turn; shock appeared at localized area
B	335.03	4.1°	Buffet onset
C	336.06	7.8°	Separation region expanded
D	337.09	12.3°	Separated flow covered the complete wing surface
E	338.12	13.9°	Recovery initiated

Table 3 Flight test run and processing information

Flight number	871, Run 2
Mach no.	0.925
Altitude	10,668m (35,000 ft)
Flap settings	(4°/12°)
Low-frequency digital tape frame rate	1000 per sec
Time increment	0.002 sec
Frequency increment	0.488 Hz
Spectral frequency range	1.4-20.0 Hz

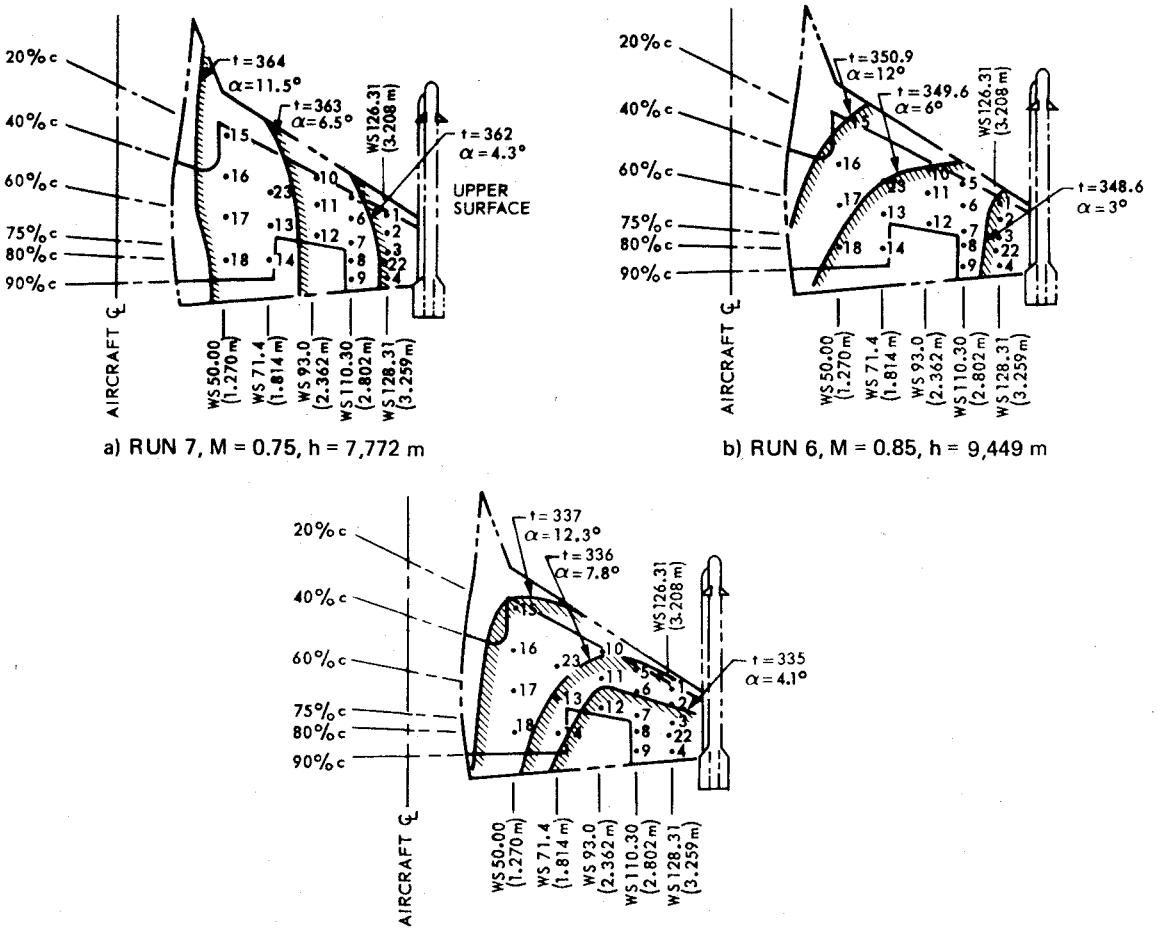

Fig. 4 Upper wing surface separation boundary mapping for three runs of flight 825, ($\delta_n/\delta_f = 0°/0°$).

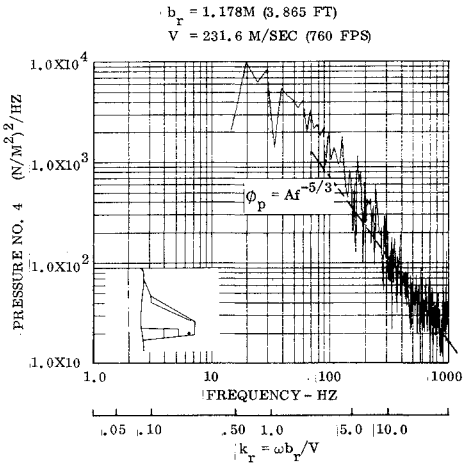

Fig. 5 Power spectrum of buffet pressure at wing station 128.31, 90% chord position, for $M_0 = 0.75$, $h = 7{,}772$ m, $\delta_n = 0°$, $\delta_f = 0°$.

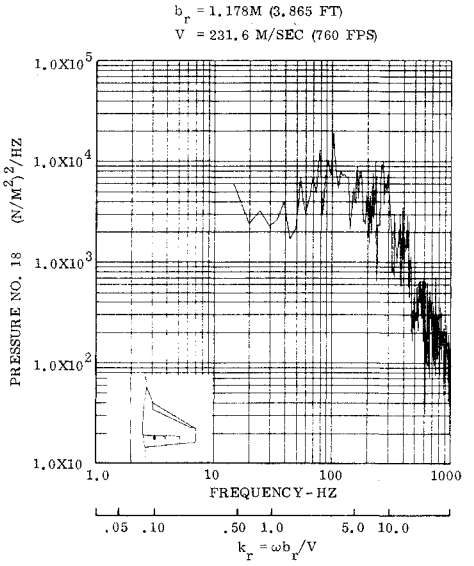

Fig. 6 Power spectrum of buffet pressure at wing station 50.00, 80% chord position, for $M_0 = 0.75$, $h = 7{,}772$ m, $\delta_n = 0°$, $\delta_f = 0°$.

where

$$[S_{p_r p_s}(\omega)]_{ij} = \frac{T}{2\pi} F_{P_{ri}}(\omega, T)\, F^*_{P_{sj}}(\omega, T) \qquad (3)$$

The aircraft modal transfer function matrix is $[H(\omega)]$, which is determined based on aircraft mass, and mass distribution, damping and stiffness data, as well as its aerodynamic characteristics. According to the nonstationary analysis or segmentwise stationary analysis, the PSD matrix of the modal coordinates α due to buffet pressure excitation defined by Eq. (2) is

$$[S_{\alpha}(\omega_1,\omega_2)] = [H(\omega_1)]\ [S_q(\omega_1,\omega_2)]\ [H^*(\omega_2)]^T$$

$$= \sum_{r=1}^{n}\sum_{s=1}^{n}\int_{-\infty}^{\infty} A_r(\omega-\omega_1)\ [H(\omega_1)]\ [X]^T \lceil A \rfloor \times [S_{p_r p_s}(\omega)]\ \lceil A \rfloor [X]\ [H^*(\omega)_2]^T A_s^*(\omega-\omega_2)\, d\omega \qquad (4)$$

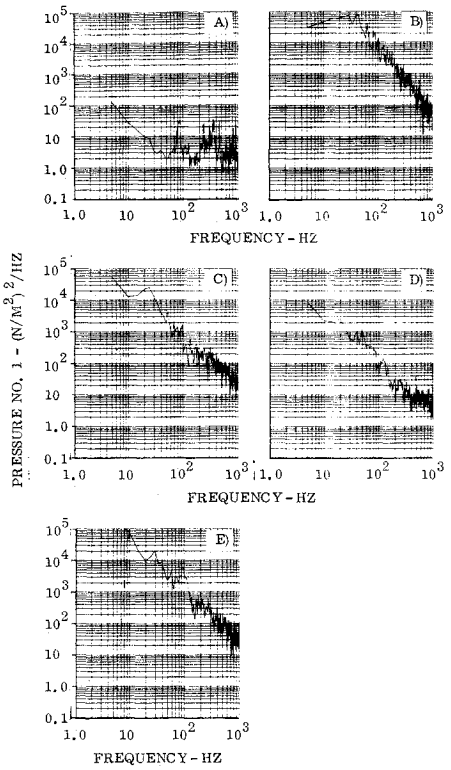

Fig. 7 PSD's of pressure no. 1 based on various segments of real time data, $M_0 = 0.925$, $h = 10{,}668$ m, $\delta_n/\delta_f = 0°/0°$.

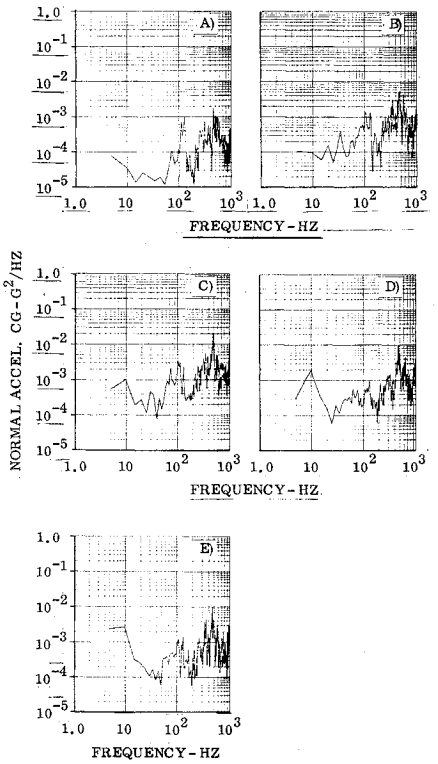

Fig. 8 PSD's of c.g. normal acceleration based on various segments of real time data, $M_0 = 0.925$, $h = 10{,}668$ m, $\delta_n/\delta_f = 0°/0°$.

where $A_r(\omega-\omega_1)$, $A_s(\omega-\omega_2)$ are the Fourier transforms of the deterministic functions defining the buffet pressure inputs in time segments r, s. Introducing a row matrix $\lfloor Y \rfloor$ which is the modal shape matrix, the PSD of deformation w at a specific location of the aircraft and the rms value of w^2 may be computed as

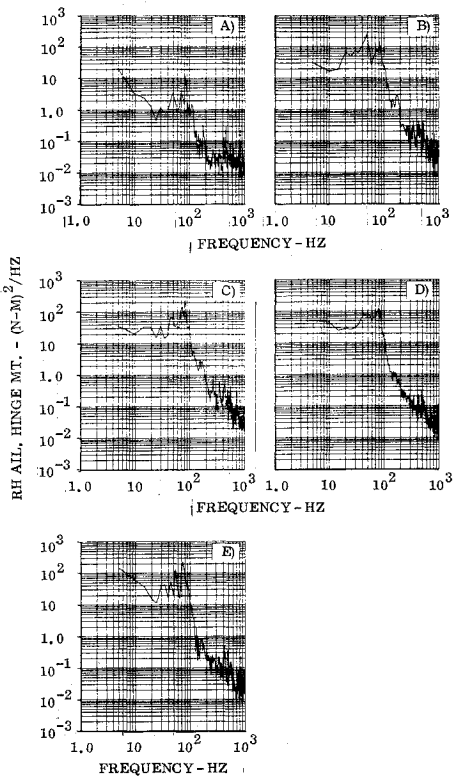

Fig. 9 PSD's of right-hand aileron hinge moment based on various segments of real time data, $M_0 = 0.925$, $h = 10{,}668$ m, $\delta_n/\delta_f = 0°/0°$.

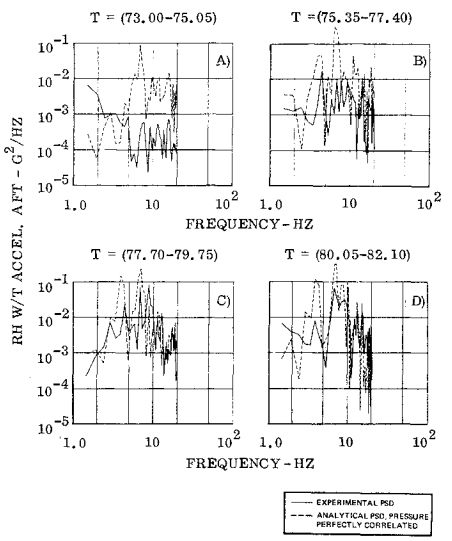

Fig. 10 Time varying PSD's of right-hand wingtip (aft) acceleration—experimental and analytical results, $M_0 = 0.925$, $h = 10{,}668$ m, $\delta_n = 4°$, $\delta_f = 12°$.

$$S_w(\omega_1, \omega_2) = \sum_{r=1}^{n} \sum_{s=1}^{n} \int_{-\infty}^{\infty} A_r(\omega-\omega_1) \lfloor Y \rfloor [H(\omega_1)] [X]^T \lceil A \rfloor [S_{p_r p_s}(\omega)] \lceil A \rfloor [X] [H^*(\omega_2)]^T \{Y\} A_s^*(\omega-\omega_2)\, d\omega \quad (5)$$

$$\overline{w^2(t)} = \int \int_{-\infty}^{\infty} S_w(\omega_1, \omega_2) \exp[i(\omega_1-\omega_2)t]\, d\omega_1\, d\omega_2 = \sum_{r=1}^{n} \sum_{s=1}^{n} \int_{-\infty}^{\infty} \lfloor Y \rfloor [I_r(t,\omega)] [X]^T \lceil A \rfloor [S_{p_r p_s}(\omega)] \lceil A \rfloor [X] [I_s^*(t,\omega)]^T \{Y\}\, d\omega \quad (6)$$

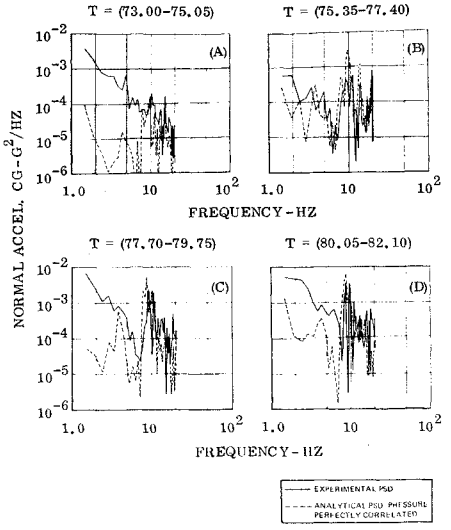

Fig. 11 Time varying PSD's of CG normal acceleration—experimental and analytical results, $M_0 = 0.925$, $h = 10{,}668$ m, $\delta_n = 4°$, $\delta_f = 12°$.

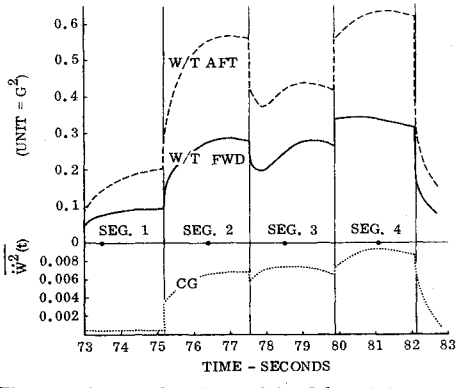

Fig. 12 Time varying accelerations of the CG and right-hand wingtip during the transonic maneuver, run 2, flight 871, $M_0 = 0.925$, $h = 10{,}668$ m, $\delta_n = 4°$, $\delta_f = 12°$.

where

$$\left(I_r(t,\omega)\right)_{ij} = \int_{-\infty}^{\infty} \left(H(\omega_l)\right)_{ij} A_r(\omega - \omega_l) \exp(i\omega_l t)\, d\omega_l \tag{7}$$

This analysis is used to compute the F-5A spectral responses based on the measured buffet pressures.[18] Using the flight test data described at the beginning of this section and the F-5A structural and aerodynamic data, the time-varying acceleration PSD's for the c.g. and the right-hand wing tip are computed at specific times, one each within the four time segments. These results are plotted in Figs. 10 and 11. Also plotted are the corresponding segmentwise stationary PSD's based on the flight test response data. For the response PSD's at the right-hand wing tip, the computed data are too high in the first segment. This is believed due to the higher damping (of the Coulomb type) of the primary structural modes at the initial phase of the maneuver not accounted for in the computation. The correlation is more satisfactory in the third and fourth segments when wing rock takes place. For the c.g. acceleration PSD's, Fig. 11, the computed first segment PSD values are low. This phenomenon may be a result of the primary structural modes contributing very little to c.g. acceleration. Assuming the available spectral energy to excite the aircraft remains constant in a fixed frequency band, an overestimate of the structural mode response may result in a corresponding underestimate of the rigid body response (the plunging mode) in the same frequency range. For the later segments, with some exceptions, a somewhat better correlation between the computed and flight test PSD data is realized. Furthermore, our experience in using the segmentwise stationary procedure seems to indicate that the computed PSD results are not overly sensitive to the way the time segments are defined within the time span of a transonic maneuver. This is understandable since the segmentwise stationary procedure is essentially an integration procedure.

In Fig. 12, the time-varying mean-square acceleration for the c.g. and the two stations of the right-hand wing tip based on the segmentwise stationary formulation are plotted. Again, only spectral contributions in the frequency range 1.4-20.0 Hz are accounted for. The figure reflects the very low c.g. response in the first time segment as described. The substantial differences in mean-square accelerations between the two wing-tip stations reveal substantial wing torsion mode participation.

Conclusions

Based on the buffet flight tests and the related analytical processing, the following conclusions may be drawn.

1) Precise and detailed dynamic pressure data acquisition for aircraft during transonic buffet is feasible and can be productive. Using the Plexiglass jacket technique, no significant adverse effect of the added instrumentation and change of airfoil geometry to the natural flow pattern was observed based on the dynamic flow development on the wing and the comparison with the tuft data. Fairly consistent mapping of the separation boundaries was achieved.

2) The pressure PSD distributions of a buffeting aircraft were such that the establishment of a mathematical model based on a number of flight condition parameters was feasible. Whether the mathematical model is general enough to cover various types or designs of aircraft is a matter subject to furture investigation.

3) Given detail buffet pressure data, the aircraft responses were predicted in the low-frequency range using linear transform function technique. The segmentwise stationary approach was the preferred approach. With additional refinements in both buffet pressure model formulation and aircraft transfer function computation, a practical method can be developed for aircraft buffet response prediction. Additional research and development work in the subject area should be most desirable and fruitful.

4) The aircraft rms load levels at c.g. and key structure locations are usually not high in a transonic maneuver as compared to the design load levels. Apparently the pilot is more aware of and sensitive to the buffet loads (longitudinal and laternal) due to the dynamic nature of the responses and the interaction with the control system.

References

[1] Huston, W. B., Rainey, A. G., and Baker, T. F., "A Study of the Correlation Between Flight and Wind-Tunnel Buffeting Loads," RM L55E16b, July 1955, NACA.

[2] Huston, W. B., and Skopinski, T. H., "Probability and Frequency Characteristics of Some Flight Buffet Loads," TN 3733, Aug. 1956, NACA.

[3] Humphreys, M. D., "Pressure Pulsations on Rigid Airfoils," RM L51112, Dec. 1951, NACA.

[4] Coe, C. F. and Mellenthin, J. A., "Buffeting Forces on Two-Dimensional Airfoils as Affected by Thickness and Thickness Distribution," RM A53K24, Feb. 1954, NACA.

[5] Chapman, D. R., Kuehn, D. M., and Larson, H. K., "Investigation of Separated Flows in Supersonic and Subsonic Streams with Emphasis on the Effect of Transition," TR-1356, 1958, NACA.

[6] Pearcy, H. H., "A Method for the Prediction for the Onset of Buffeting and Other Separation Effects from Wind Tunnel Tests on Rigid Models," ARC 20631, AGARD Rept. 223, Oct. 1958, Aeronautical Research Council, London.

[7] Mabey, D. G., "Comparison of Seven Wing Buffet Boundaries Measured in Wind Tunnel and in Flight," C.P. 840, Sept. 1966, Aeronautical Research Council, London.

[8]Blackwell, J. A. Jr., "Effect of Reynolds Number and Boundary-Layer Transition Location on Shock-Induced Separation," TN D-5003, Dec. 1968, NASA.

[9]Cahill, J.F. and Cooper, B.L., "Flight Test Investigation of Transonic Shock-Boundary Layer Phenomena," AFFDL TR-68-84, July 1968, Air Force Flight Dynamics Lab., Wright Patterson Air Force Base, Ohio.

[10]Titiriga, A. Jr., "F-5A Transonic Buffet Flight Test," AFFDL-TR-69-110, Oct. 1969, Air Force Flight Dynamics Lab., Wright-Patterson Air Force Base, Ohio.

[11]Fischel, J. and Friend, E. L., "Preliminary Assessment of Effects of Wing Flaps on High Subsonic Flight Buffet Characteristics of Three Airplanes," TM X-2011, May 1970, NASA.

[12]Damstrom, E. K. and Mayes, J. F., "Transonic Flight and Wind Tunnel Buffet Onset Investigation of the F-8D Aircraft, *Journal of Aircraft,* Vol. 8, April 1971, pp. 263-270.

[13]Hollingsworth, E. G. and Cohen, M., "Determination of F-4 Aircraft Transonic Flight Buffet Characteristics," *Journal of Aircraft,* Vol. 8, Oct. 1971, pp. 757-763.

[14]Cohen, M., "Buffet Characteristics of the Model F-4 Airplane in the Transonic Flight Regime," AFFDL-TR-70-56, April 1970, Air Force Flight Dynamics Lab., Wright-Patterson Air Force Base, Ohio.

[15]Mullans, R. E. and Lemley, C. E., "Buffet Dynamic Loads During Transonic Maneuvers," AFFDL-TR-72-46, July 1972, Air Force Flight Dynamics Lab., Wright-Patterson Air Force Base, Ohio.

[16]Townsend, A. A., *The Structure of Turbulent Shear Flow,* Cambridge Univ. Press, New York, 1956.

[17]Bendat, J. A. and Piersol, A. G., *Measurement and Analysis of Random Data,* Wiley, New York, 1966.

[18]Hwang, C. and Pi, W. S., "Investigation of Northrop F-5A Wing Buffet Intensity in Transonic Flight," Rept. CR-2484, Nov. 1974, NASA.